GEOPHYSICS, VOL. 63, NO. 2 (MARCH-APRIL 1998); P. 431–439, 13 FIGS.

Separation of regional and residual magnetic field data

Yaoguo Li* and Douglas W. Oldenburg*

ABSTRACT

We present a method for separating regional and residual magnetic fields using a 3-D magnetic inversion algorithm. The separation is achieved by inverting the observed magnetic data from a large area to construct a regional susceptibility distribution. The magnetic field produced by the regional susceptibility model is then used as the regional field, and the residual data are obtained by simple subtraction. The advantages of this method of separation are that it introduces little distortion to the shape of the extracted anomaly and that it is not affected significantly by factors such as topography and the overlap of power spectra of regional and residual fields. The proposed method is tested using a synthetic example having varying relative positions between the local and regional sources and then using a field data set from Australia. Results show that the residual field extracted using this method enables good recovery of target susceptibility distribution from inversions.

INTRODUCTION

Magnetic data observed in geophysical surveys are the sum of magnetic fields produced by all underground sources. The targets for specific surveys are often small-scale structures buried at shallow depths, and the magnetic responses of these targets are embedded in a regional field that arises from magnetic sources that are usually larger or deeper than the targets or are located farther away. Correct estimation and removal of the regional field from the initial field observations yields the residual field produced by the target sources. Interpretation and numerical modeling are carried out on the residual field data, and the reliability of the interpretation depends to a great extent upon the success of the regional-residual separation. Few papers, however, deal specifically with this issue. Most of the work is concerned with gravity data, but many of the methods can be extended to magnetic data processing. A comprehensive review of these methods can be found in Hinze (1990), but the methods generally fall into one of the following four categories. The simplest is the graphical method in which a regional trend is drawn manually for profile data. Determination of the trend is based upon the interpreter's understanding of the geology and the related field distribution. This is a subjective approach and also becomes increasingly difficult with large 2-D data sets. In the second approach, the regional field is estimated by least-squares fitting a low-order polynomial to the observed field (Agocs, 1951; Oldham and Sutherland, 1955; Skeels, 1967). This reduces subjectivity, but one still needs to specify the order of the polynomial and to select the data points to be fit. The third approach applies a digital filter to the observed data to separate the long wavelength anomalies associated with the regional field from the shorter wavelength anomalies associated with the target structure. In the spatial domain, this is achieved by convolving the observed field with a set of filter coefficients (e.g., Griffin, 1949), but the computation is more efficiently carried out in the wavenumber domain where the Fourier transform of the observations is multiplied by a zero-phase transfer function (e.g., Zurflueh, 1967; Gupta and Ramani, 1980; Pawlowski and Hansen, 1990; Pawlowski, 1994). Because the wavenumber-domain approach is very efficient and easy to accomplish, it has become a popular method for regional-residual separation. Both simple band-pass filters and Wiener optimum filters have been used. The latter can incorporate knowledge about geology through the estimation of the power spectra of the different components (either regional or residual field, or both) (Pawlowski and Hansen, 1990). The fourth approach is a stripping method based upon detailed geological information in which the field of known geological units is calculated and subtracted from the observations. Hammer (1963) used this method to extract the signal of deep sources by removing the modeled shallow responses. Although that work has a very different emphasis compared to the problem of regional-residual separation, the principle still stands and represents an interesting approach to the problem.

Of the four methods mentioned, the first three have two common drawbacks. First, they all implicitly assume that the

Presented at the 65th Annual International Meeting, Society of Exploration Geophysicists. Manuscript received by the Editor June 10, 1996; revised manuscript received June 3, 1997.
*Dept. of Earth and Ocean Sciences, University of British Columbia, 2219 Main Mall, Vancouver, B. C. V6T 1Z4, Canada. E-mail: li@geop.ubc.ca; doug@geop.ubc.ca.

regional field is smooth. However, when the observations are located on a topographic surface, the assumption of smoothness is rendered inaccurate. LaFehr and MacQueen (1990) provide a lucid illustration of this problem. Second, these methods invariably tend to distort the shape of the extracted residual anomalies. Underlining this tendency is the fact that the regional fields estimated in these methods do not necessarily correspond to the fields that might be produced by geophysically plausible sources. The most apparent distortion is the dc shift and change in anomaly width resulting from band-pass filtering. Because of the distortion, the extracted anomalies are often useful for tasks such as structural mapping or qualitative interpretation based on visual inspection of the data, but they are not suitable for quantitative modeling and inversion. The difficulty becomes more apparent when the anomaly to be extracted is located beside a shallow regional source. We illustrate this with a data set generated from a synthetic model that consists of a small dipping dyke situated above a deep regional source and beside a shallow regional source. Figure 1 displays one plan-section and two cross-sections of the model. Given an inducing field in the direction $I = 65°$ and $D = 25°$, the model produces the total field anomaly on the surface that is shown in Figure 2. The data are simulated at 25-m intervals along north-south lines spaced 50 m apart and have been contaminated by uncorrelated Gaussian noise having zero mean and a standard deviation of 5 nT. That data map shows a commonly occurring situation where the anomaly of interest is superimposed upon a slowly varying field and, at the same time, is on the flank of an adjacent large anomaly. We seek to extract (in the area marked by the dashed lines) the residual anomaly caused by the dipping dyke. It is not possible to do this with standard filtering techniques. The resulting residual data might be a clear enough image of the anomaly so that qualitative interpretation may be carried out; however, details will be lost, and the extracted anomaly will be contaminated severely by the field from the large shallow block. An inversion using such data may not produce sensible models.

In contrast to the filtering approach, the stripping method is based on the known geological structure, and the extracted anomalies are therefore expected to correspond to geologically meaningful magnetic sources. For the purpose of inversion, the stripping method is a more suitable approach for residual separation. However, the lack of reliable information about the magnetic sources to be removed prohibits its use in most practical cases.

The above methods for regional-residual separation have been successfully incorporated into the processing and interpretation of magnetic data. Because of their limitations, however, they have not always met our needs for processing data that are to be inverted to recover magnetic susceptibility distributions. In this paper, we adopt the principle of the stripping method and develop a different approach to the problem of regional-residual separation by applying a 3-D magnetic inversion algorithm to magnetic data on multiscales. In the following, we first outline the procedure for the separation and then illustrate it with synthetic examples. We then apply it to a set of field data and conclude the paper with a brief discussion.

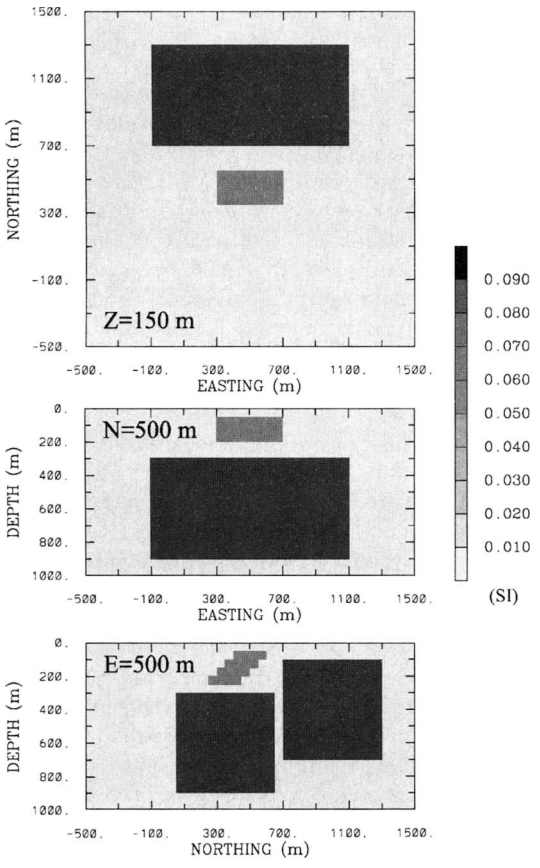

FIG. 1. The susceptibility model consists of a dipping dyke as a local source that is situated above a deep regional source and beside another regional source at a shallow depth. This model typifies the two relative positions between the local and regional source, i.e., they are either vertically or laterally displaced from each other. The susceptibility is given in SI units.

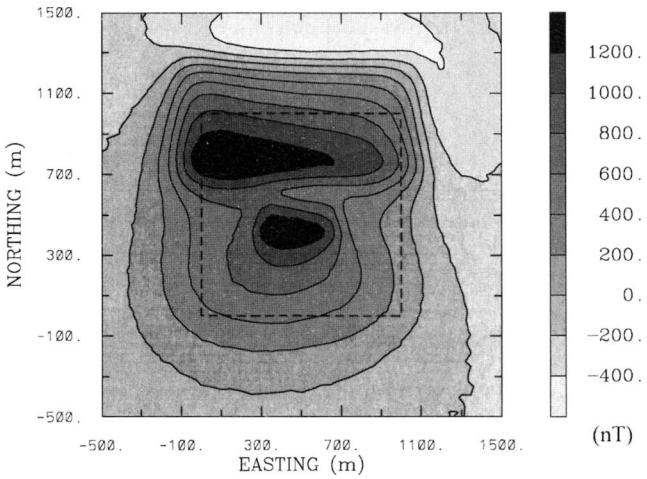

FIG. 2. The total magnetic field (in nanoteslas) produced by the susceptibility model shown in Figure 1. The assumed inducing field is in the direction $I = 65°$, $D = 25°$. The data are contaminated by uncorrelated Gaussian noise with a standard deviation of 5 nT. The field produced by the dipping dyke is superimposed upon the slowly varying field of the deep source, and it is situated on the flank of the field of the shallow regional source. The objective is to separate the residual field due to the dyke from the regional field in the central area marked by the dashed lines.

INVERSION FOR REGIONAL SOURCES

We seek to formulate a method for separating the regional and residual field components in a given magnetic data set. The residual data will be subjected to further quantitative analyses; hence, they need to be reproducible by geologically reasonable models located within the region of interest. This requires that the separation algorithm preserves characteristics of the anomalies such as the ratio of positive to negative peak value, the width of the anomaly, and the dc component within the finite data area. Thus the regional field to be subtracted must arise from a physical distribution of magnetic susceptibility. To find that susceptibility, we use the 3-D magnetic inversion algorithm of Li and Oldenburg (1996).

The inversion algorithm has been developed to invert surface magnetic data for 3-D distributions of magnetic susceptibilities and is applicable to problems on different scales. Readers are referred to the original paper for details; we only summarize the essentials here. The algorithm assumes that the measured magnetic field is produced only by induced magnetization, that no remanent magnetization is present, and that the demagnetization effect is negligible. The susceptibility distribution is represented by a large number of rectangular cells of constant susceptibility, and the final solution is obtained by finding a model that reproduces the data adequately and at the same time minimizes a model objective function penalizing the structural complexity of the model. A depth weighting function of the form $w(z) = (z + z_0)^{3/2}$ is applied to counteract the decay of sensitivity and distribute the recovered susceptibility with depth (where z is the depth of the cell and z_0 is a constant dependent upon the observation height and model discretization). The depth weighting is crucial if the algorithm is to place the causative bodies at approximately the correct depth. Both synthetic and field data sets have been used to test the performance of the inversion algorithm.

In this paper, we use this algorithm in a multiscale approach to the inversion of magnetic data. The process simultaneously achieves the required regional-residual separation. To effect the regional-residual separation, we proceed as follows. Let S_L be the area in which one intends to extract the residual data that are produced by the local sources in a volume V_L directly below. Let S_R be a larger area that encloses S_L. The separation begins by defining a mesh for the regional model in volume V_R that is beneath S_R and encloses V_L. The relation between these regions is shown in Figure 3. The mesh for this model is coarse and can only represent large-scale susceptibility variations. As a first step, the data in S_R are down-sampled to form the data for regional inversion. This serves both to produce a data set consistent with the regional model and to limit the size of the corresponding inverse problem. Inverting these data produces the large-scale susceptibility distribution in V_R. We then determine the local source volume V_L and set the susceptibility in this region to zero to form the regional susceptibility model κ_R. This model represents all the non-local sources, and its forward modeled response forms the regional field in the area S_L. The residual field is obtained by subtracting this field from the initial observations. The derived residual field can then be used in the subsequent inversion to generate a more detailed model of susceptibility in V_L.

The above description outlines the general steps of the algorithm. Its practical implementation requires the specification of a number of parameters. These include the cell size for the regional model, interval of the regional data and the method of down-sampling, and choice of the local source volume in the calculation of regional field. These parameters will be problem dependent, but general criteria are provided below.

The cell dimensions for the regional model should be two to five times that intended for the inversion of the residual data. Smaller cells will make the regional inversion effectively a detailed inversion on an unnecessarily large scale, whereas too large a cell size will not provide the resolution needed for the separation. Once the cell size is chosen, the regional data can be formed by down-sampling the original observations to an interval that is the same as the width of cells. This is usually done after the data are continued upward to a height comparable to the width of the model cells, especially when there are near-surface contaminations.

The need to determine the local source region V_L introduces a subjectivity into the process, because the extracted residual data is affected by the choice of the volume V_L. However, although the choice of V_L is important, it is not crucial. As we shall illustrate with synthetic and field examples in the following sections, the horizontal boundaries of V_L can usually be determined straightforwardly based upon the recovered susceptibility. The main ambiguity is the bottom depth, because that is the direction magnetic inversions have the least resolution. If, from the regional inversion, there is a clear separation in depth between local and regional sources, then the bottom of V_L should be placed there. Otherwise, the interpreter needs to exercise judgement and incorporate any known geologic information. It may also be helpful to perform the separation using several trial depths for V_L and then examine the results. The definition of regional and residual fields is, after all, relative, and their distinction is blurred when the vertical separation between two bodies is small. Viewed as an advantage, indeterminacy in the division between the local and regional source volume offers flexibility for the interpreter to select a specific region for detailed investigation and to relegate the remainder

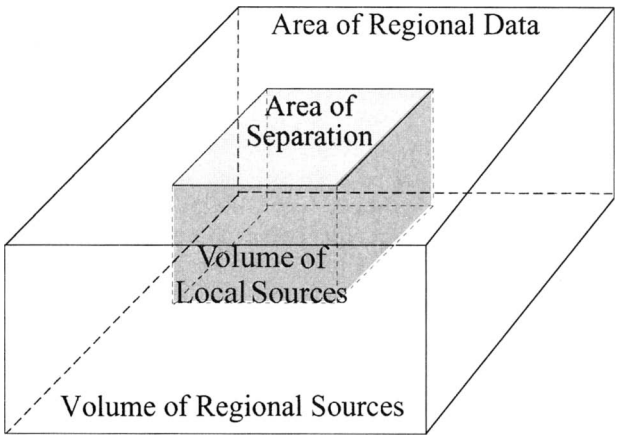

FIG. 3. The different regions used in the regional-residual separation. The outer box indicates the 3-D region used in the regional inversion. Within this region, the shaded inner box is the assumed volume of local source. Excluding the susceptibility in this region from the model recovered by the regional inversion yields the regional source for the area of field separation.

to the regional. It also allows the use of available geologic information to determine more objectively the division between local and regional sources.

Since the method achieves the separation by using the components of magnetic sources, it bears a resemblance to Hammer's (1963) stripping method of field separation discussed in the Introduction. In our method, the source parameters of the field to be removed are obtained from inversion, whereas in Hammer's method they are obtained from more direct approaches such as drilling. In this sense, our approach is an inversion-based stripping method. From a different perspective, our method is a multiscale inversion of the magnetic data. The inversion proceeds from a large scale to smaller scales, and the susceptibility recovered on one scale is used at the next smaller scale to define residual data which are then inverted for more detailed structures. This can be a useful approach for attacking data sets covering large areas.

SYNTHETIC EXAMPLES

We now illustrate our method for regional-residual field separation with a synthetic example. The two basic relative positions between local and regional sources are (1) the regional source is entirely below the local source, and (2) the regional source is beside the local source and has potentially a shallow depth to the top. More complicated situations can be formed by combining these two geometries. In the following, we focus on the example shown in Figure 1, which is one of the simplest combinations of the two geometries and consists of sources located below and to the side of a local source.

The local source is a dipping dyke that has a width of 200 m and extends from 50 to 250 m depth at a dip angle of 45°. The deep regional source extends from 300 to 900 m in depth. There is only a 50-m vertical separation between the two sources. The shallow regional source is separated from the local source horizontally by 100 m. The susceptibility is 0.05 (SI units) for the local source and 0.08 for both regional sources. The inducing field has direction $I = 65°$ and $D = 25°$, and the total field data produced on the surface are shown in Figure 2. The data, simulated at 25-m intervals along north-south lines spaced 50 m apart, have been contaminated by uncorrelated Gaussian noise. The magnetic anomaly due to the shallow dyke is seen superimposed upon a more slowly changing background produced by the regional sources. Our goal is to extract the field caused by the shallow source in the area marked by the dashed lines. The data are reproduced in Figure 4, which also shows the true regional and the residual fields for this area.

Since there is no contamination from near-surface sources, we choose not to continue the data upward, and we work with them on the original observation level. We first down-sample the data to 100 m intervals in both directions and invert them to recover a large-scale susceptibility distribution in the 2000 × 2000 × 1000 m volume that has been discretized using 100 × 100 m cells with a thickness of 50 m. The resultant model is shown in Figure 5 in one plan-section and two cross-sections. Comparison with Figure 1 shows that the large susceptibility blocks are reasonably well reproduced.

To obtain a regional susceptibility model, we first define a local source volume. The horizontal boundary is easy to choose since the local source is well separated from the regional source. We choose the local source volume to be a rectangular volume that covers horizontally from 200 to 800 m in easting and 300 to 700 m in northing and extends from surface to some depth. The separation between local and regional sources in the depth direction was only 50 m. The smooth regional inversion does not indicate the break, so the depth boundary of the local source cannot be chosen definitively. We have examined the separation results from three different depths at $z = 250, 350, 450$ m.

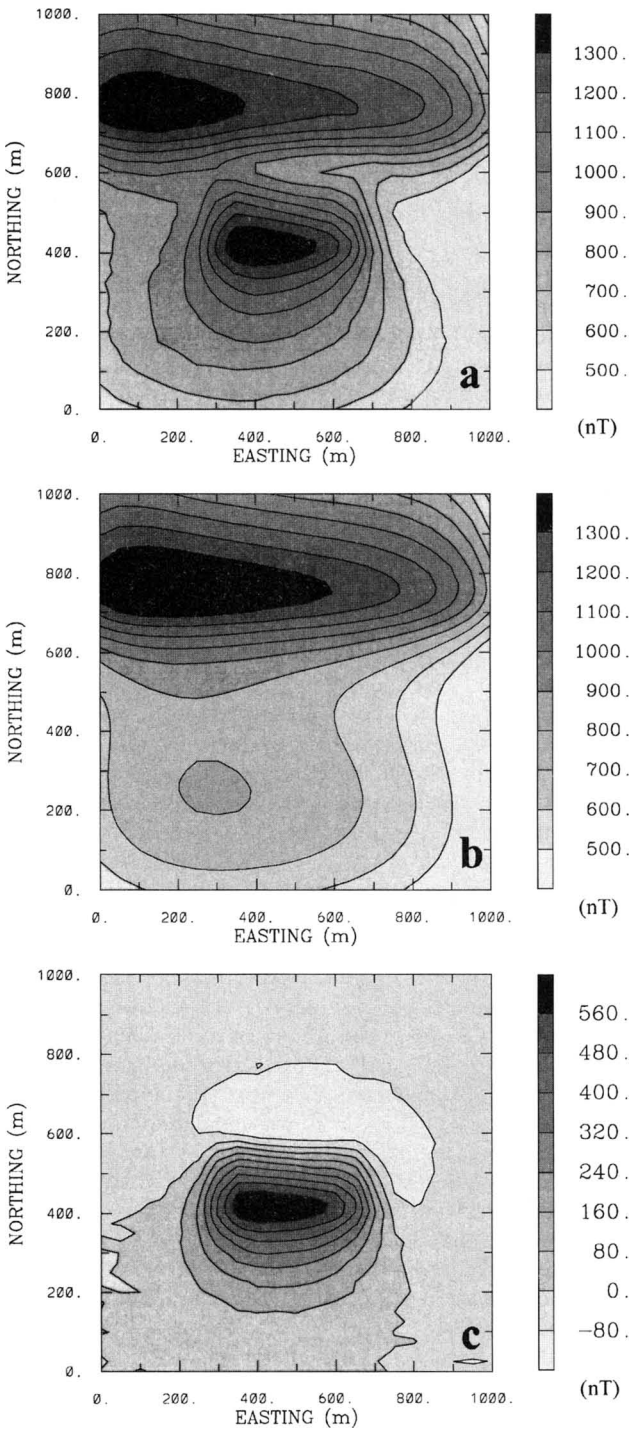

FIG. 4. The observed data (a), true regional (b), and residual field (c) in the central area shown in Figure 2. For the purpose of display, the regional field is the true field produced by the regional sources, whereas the residual field includes the additive noise.

The boundaries of the region are denoted by the solid and dashed lines in Figure 5. For each choice, we set the susceptibility in the local source region to zero, calculate a regional field from the remaining susceptibility, and subtract it from the original data in the area of interest. The resultant residual fields corresponding to the different choice of depths are shown in Figure 6. They can be compared with the residual fields shown in Figure 4. The amplitude and width of the extracted residual field increase as deeper susceptibilities are taken as local sources, but the characteristics of the residual fields are similar.

Next, we invert each of the extracted residual fields to recover a detailed local susceptibility model. The inversions use a model mesh that horizontally has the same area as the residual data map and extends to a depth of 500 m. Note that this region is larger than the volume in which the susceptibility from regional inversion is set to zero in Figure 5. (It is generally a good practice to allow the model in the inversion of the residual data to extend beyond the boundary used in the regional-residual separation so that the residual inversion is not restricted by the model parametrization.) We have divided the model into 50-m cubic cells. The recovered models are shown in the cross-section at easting = 500 m in Figure 7. Superimposed

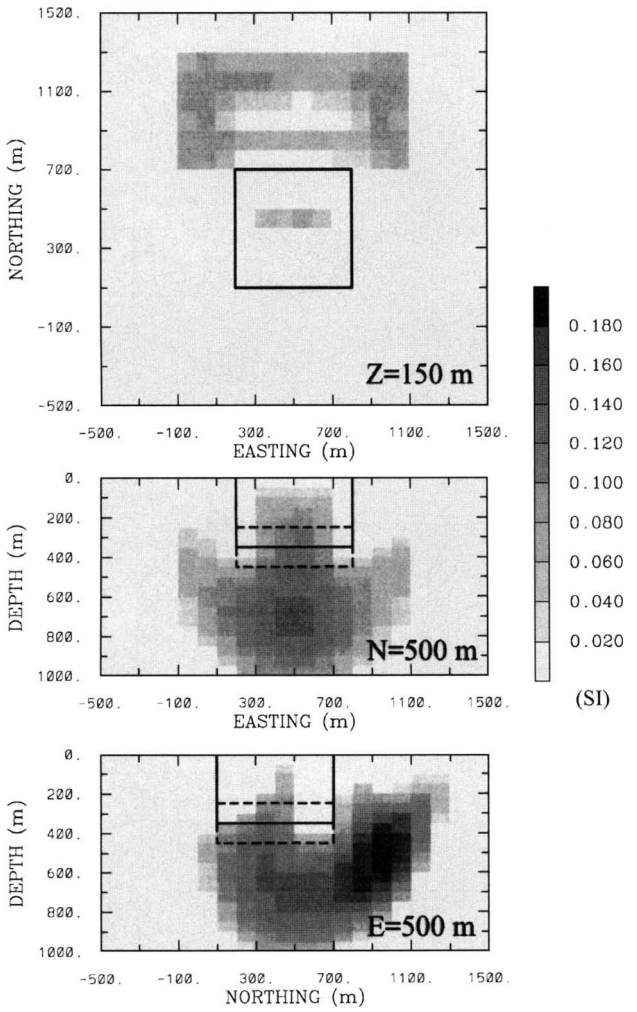

FIG. 5. The susceptibility model recovered from the regional inversion. The cells inside the rectangular volume bounded by the black lines are ascribed to the local source. Three different depths to the bottom of local source are examined. These depths are indicated in the two cross-sections by the solid horizontal line and two dashed lines. In each case, the cells outside this region are used as the regional source whose field constitutes the estimated regional field.

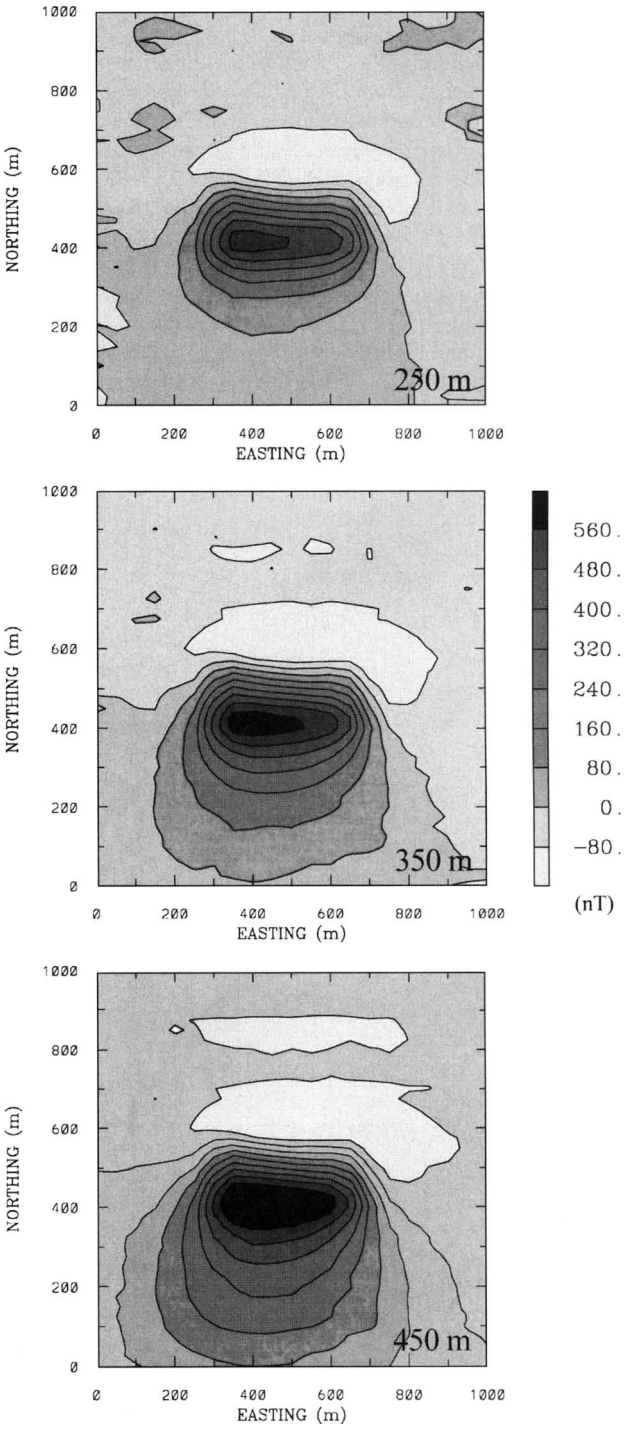

FIG. 6. The estimated residual fields obtained by subtracting from the data in Figure 2 the regional fields calculated using the regional susceptibility models shown in Figure 5. The three panels correspond, respectively, to the result obtained when the bottom of the local source is taken as 250, 350, and 450 m.

on each section is the true boundary of the dipping dyke. The upper portion of the dyke is well delineated by all three models. The recovered susceptibility extends to increasing depth as the assumed bottom depth of local source increases in the separation process. This is to be expected. The comparison in Figure 7 demonstrates that the choice of local source volume during the calculation of regional field is an important factor that will change the extracted residual field, but it is not crucial for the final interpretation.

Without independent information regarding the susceptibility distribution that might be available in field applications, it is difficult to choose among the three models in Figure 7. However, examination of Figure 5 would suggest that a depth of 450 m is probably too deep since it is well within the broad susceptibility that extends to greater depths. The model obtained using the depth of 350 m is shown in one plan-section and two cross-sections in Figure 8. We note that, when plotted in the same format, the other two models display the same horizontal extent of the susceptibility high in the plan section. The depth extent in section northing = 500 m is slightly shallower for the first model and slightly deeper for the third model. Overall, they all delineate the dipping dyke reasonably well, and one would obtain the same interpretation from any of the three models.

FIELD EXAMPLE

As the second example, we invert a set of aeromagnetic data acquired in Australia. The total field data were recorded every 8.5 m on average along flight lines with a mean spacing of 80 m. The data were collected at a terrain clearance of 50 m in a flat area, and the geomagnetic field in the area is in the direction $I = -65.43°$, $D = 0.55°$. Figure 9 displays the original data, which cover an area of 1000 × 1000 m. The scale bar indicates the value of the observation after the international geomagnetic reference field (IGRF) is removed. The main features in this map are the high positive anomaly toward the south, a localized anomaly at the north, and a small anomaly in the center that is manifested by a distortion of the contour line. This latter feature is the anomaly of interest to the exploration project. In this case, we carry out the regional removal in the 600 × 500 m area marked by the dashed lines and invert the resulting residual data to produce a susceptibility model.

The IGRF-removed data are mostly negative, and the nature of the negative shift is unknown. However, for the purpose of

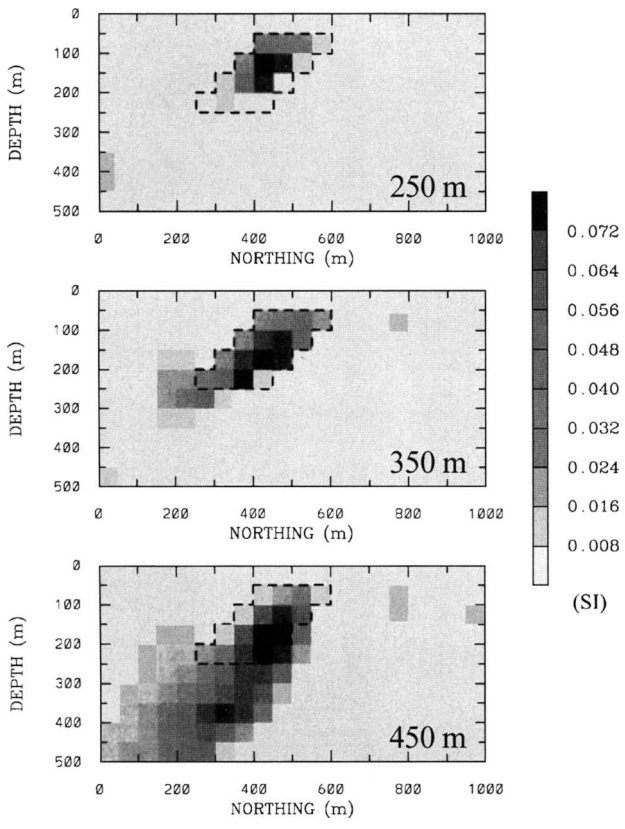

FIG. 7. The susceptibility models recovered by inverting the extracted residual data shown in Figure 6. Each model is displayed in cross-section at easting = 500 m. The label in each panel indicates the bottom depth of local source used in the separation. All three recovered models image the dipping dyke reasonably well, as indicated by the overlaid outline of the dyke (dashed lines).

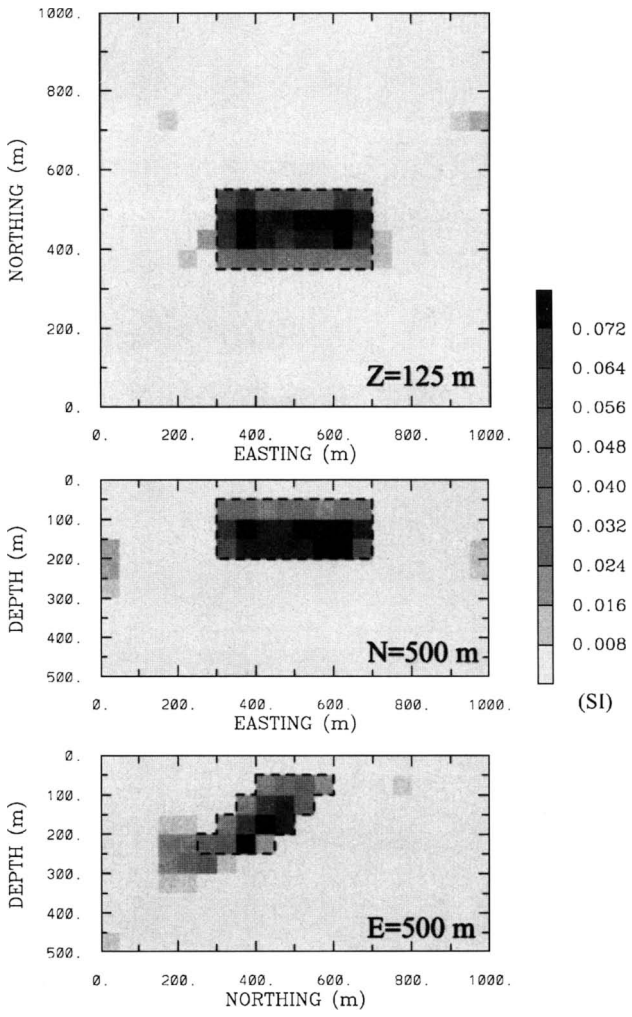

FIG. 8. The susceptibility model recovered by inverting the residual field when the bottom depth of local source is assumed to 350 m. The model is displayed here in one plan-section at $z = 125$ m and two cross-sections respectively at northing = 500 m and easting = 500 m. The dipping dyke is well imaged in all directions.

regional-residual separation, it is of minor concern. To use the positivity constraint in the 3-D magnetic inversion algorithm during the regional inversion, we first add 400 nT to the entire data set. This added shift is chosen arbitrarily, and it allows the recovery of a positive susceptibility model. The shifted data are then down-sampled along flight lines, and every tenth point is retained as regional data. The model for the regional inversion covers an area of 1.7 × 1.7 km and extends to a depth of 1 km. The cells in the center have a width of 100 m in both horizontal directions and the thickness ranges from 25 m near the surface to 200 m at the bottom. The inversion produces a model that fits the down-sampled data to 3 nT on average. The central portion of the susceptibility model recovered from the regional inversion is shown in three sections in Figure 10. As outlined by the dashed lines, the regional source is taken to be outside a volume extending from 6000 to 6350 m in easting, from 5500 to 5900 m in northing, and from surface to 250 m in depth. Using this regional susceptibility model, we calculate the regional field for the area of separation as shown in Figure 11(a). The residual field obtained after removing the regional from the data in Figure 9 is shown in Figure 11(b).

When the residual data in Figure 11(b) are inverted, we recover a 3-D susceptibility model for the local source. The model, shown in Figure 12, is displayed in one plan-section, one cross-section, and one longitudinal section. It shows a zone of high susceptibility at a depth of 100 m. A comparison of the recovered susceptibility model with the susceptibility log from drill cores is provided in Figure 13. The center of the inverted anomaly coincides with high magnetic susceptibility values from the drill log. This comparison shows that our method of regional-residual separation has yielded an estimate of the residual data that is consistent with the local source and, therefore, the separation procedure has been successful.

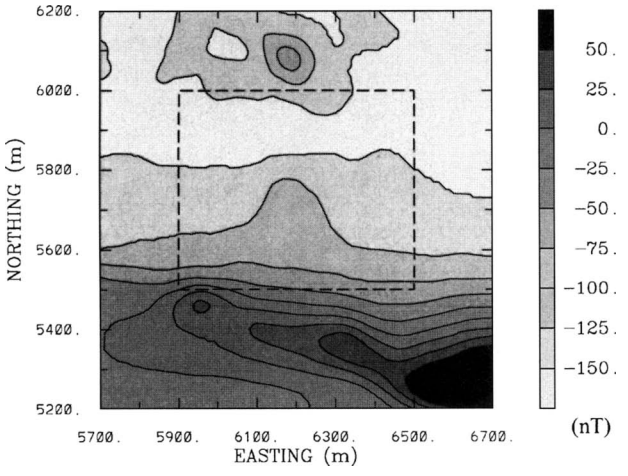

FIG. 9. The total field aeromagnetic data collected in Australia. The direction of the geomagnetic field in the area is $I = -65.43°$ and $D = 0.55°$. The data have a fairly constant height of 50 m above the ground surface. The gray scale indicates the value of the observation after the IGRF is removed. The anomaly of interest (in the center of the figure) is located on the flank of major regional field caused by a body at the south end. We seek to extract the anomaly in the 600 × 500 m area outlined by the dashed lines.

DISCUSSION

We have developed a new method for separating regional and residual components of magnetic data. It is based upon the 3-D inversion of magnetic data on different scales. The inversion at a large scale produces a regional distribution of susceptibility, and the susceptibilities outside a user-determined local source region are then used to define the regional field for the area above this local region. Removal of this regional field from the initial observation yields the desired residual data that can be inverted to recover detailed susceptibility variation. Applications to synthetic and field data sets have produced good results and demonstrated the flexibility of the method.

Compared with the commonly used techniques such as wavenumber filtering, this approach has several advantages. First, it does not rely solely on the power spectra of the regional and residual fields and, therefore, is much less affected by their overlap. Second, the extracted residual field is always physically plausible since the regional field is calculated from a distribution of susceptibility. Such physical realizability is not

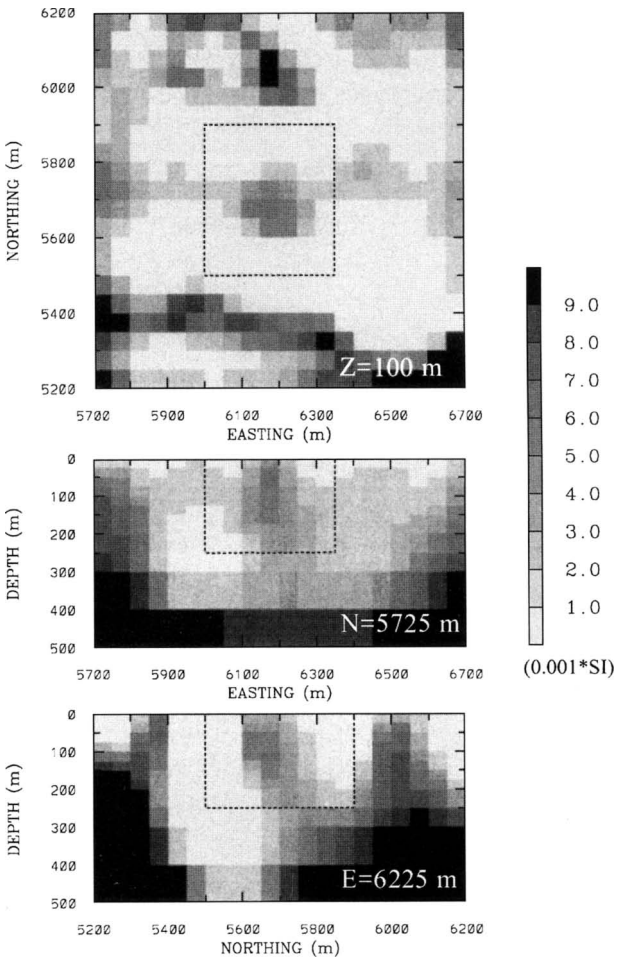

FIG. 10. The susceptibility model recovered from the regional inversion is shown in one plan-section and two cross-sections. Only the central portion of the model is shown here for clarity. The gray scale indicates the susceptibility value in 10^{-3} SI units. The susceptibilities outside the volume marked by the dashed lines are taken as the regional susceptibility for calculating the estimated regional field in the area indicated in Figure 9.

guaranteed for the residual field derived using traditional techniques. Third, this method of separation is applicable generally for data sets with arbitrary observation locations. For example, the data can be located on the original flight lines. When the data are located along a topographic surface, this method will be superior to traditional methods in modeling the rapid change in the regional field due to the change in the observation height. Of course, these advantages are obtained with cost. The biggest hurdle in the application of this method is the required computation, which is many orders of magnitude greater than that for applying polynomial fitting or filtering. Since the inversion algorithm assumes induced magnetization, this method is expected to have difficulties when strong remanent magnetization is present. Also, the method is not completely objective in that the user still needs to choose the local source volume, but this task seems to be easier than choosing filter parameters and it might be accomplished more objectively.

Given its relative strength, our work complements the existing methods of field separation and overcomes some of their shortcomings. It will produce a residual field of the quality necessary for quantitative modeling and inversion and thus will be most useful in the final, quantitative interpretation of a data set. This approach to field separation is also expected to lend itself to the processing and inversion of data sets for which large-scale variations of susceptibility are inverted for the area as a whole, and detailed structures are recovered only for specific areas of interest.

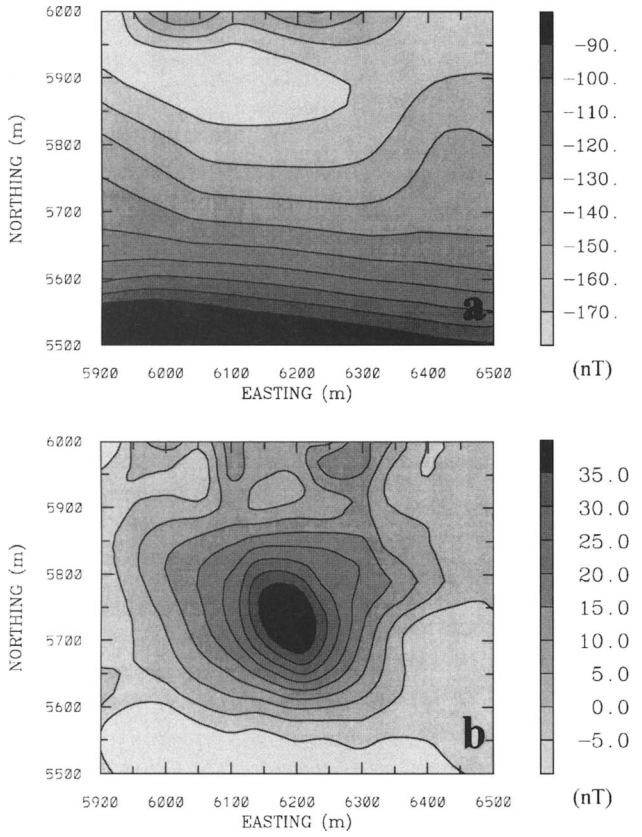

FIG. 11. Panel (a) is the estimated regional field for the area of interest. The subtraction of this regional field from the initial field data in Figure 9 yields the residual data displayed in panel (b).

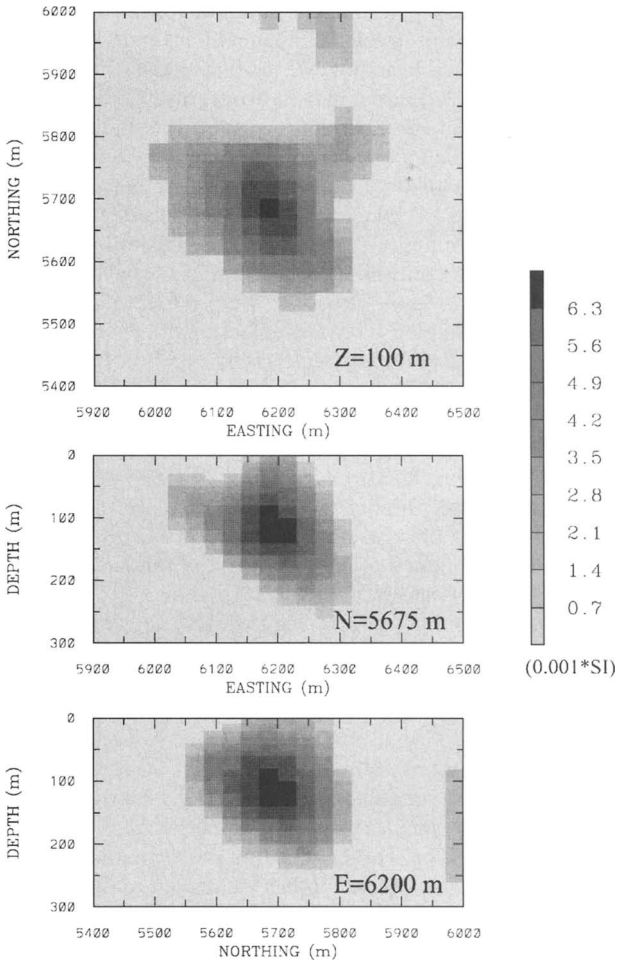

FIG. 12. The susceptibility model recovered by inverting the extracted residual data shown in Figure 11(b). The gray scale indicates the susceptibility value in 10^{-3} SI units. The model shows a well-defined susceptibility high centered at a depth of about 100 m.

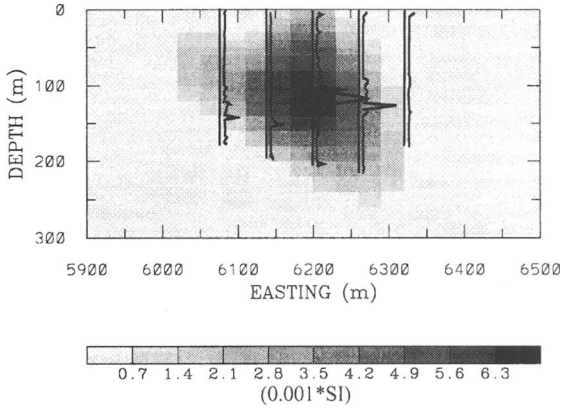

FIG. 13. Comparison of the susceptibility from the inverted model (gray shading) and the susceptibility from drill logs in the cross-section at northing = 5675 m. The inverted susceptibility (shown by the gray scale) has units of 10^{-3} SI. The value of the drill log is relative and only indicates zones of high susceptibility.

ACKNOWLEDGMENTS

This work was supported by an NSERC IOR grant and an industry consortium "Joint and Cooperative Inversion of Geophysical and Geological Data". Participating companies are Placer Dome, BHP Minerals, Noranda Exploration, Cominco Exploration, Falconbridge, INCO Exploration & Technical Services, Hudson Bay Exploration and Development, Kennecott Exploration Company, Newmont Gold Company, Western Mining Corporation, and CRA Exploration Pty. We also thank D. Johnson and Western Mining Corporation for supplying the field data set.

REFERENCES

Agocs, W. B., 1951, Least-squares residual anomaly determination: Geophysics, **16**, 686–696.

Griffin, W. P., 1949, Residual gravity in theory and practice: Geophysics, **14**, 39–56.

Gupta, V. K., and Ramani, N., 1980, Some aspects of regional residual separation of gravity anomalies in a Precambrian terrain: Geophysics, **45**, 1412–1426.

Hammer, S., 1963, Deep gravity interpretation by stripping: Geophysics, **28**, 369–378.

Hinze, W. J., 1990, The role of gravity and magnetic methods in engineering and environmental studies, *in* Ward, S. H., Ed., Geotechnical and environmental geophysics, **1**, 75–126.

LaFehr, T. T., and MacQueen, J. D., 1990, Regional-residual separation in rugged topography: 60th Ann. Intern. Mtg., Soc. Expl. Geophys., Expanded Abstracts, 620–622.

Li, Y., and Oldenburg, D. W., 1996, 3-D inversion of magnetic data: Geophysics, **61**, 394–408.

Oldham, C. H. G., and Sutherland, D. B., 1955, Orthogonal polynomials and their use in estimating the regional effect: Geophysics, **20**, 295–306.

Pawlowski, R. S., 1994, Green's equivalent-layer concept in gravity band-pass filter design: Geophysics, **59**, 69–76.

Pawlowski, R. S., and Hansen, R. O., 1990, Gravity anomaly separation by Wiener filtering: Geophysics, **55**, 539–548.

Skeels, D. C., 1967, What is residual gravity?: Geophysics, **32**, 872–876.

Zurflueh, E. G., 1967, Application of two-dimensional linear wavelength filtering: Geophysics, **32**, 1015–1035.